13th World Conference on Earthquake Engineering
Vancouver, B.C., Canada
August 1-6, 2004
Paper No. 3366

SEISMIC ISOLATION SYSTEM WITH CONVERTIBLE ACTIVE AND PASSIVE MODES USING LINEAR MOTORS FOR MONOCRYSTAL PULLERS

Hironori FURUKAWA[1], Takafumi FUJITA[2], Takayoshi KAMADA[3], Shichihei SAKURAGI[4], and Hideaki MISOKA[5]

SUMMARY

This paper describes a seismic isolation system for monocrystal pullers. In the monocrystal puller, a monocrystal is suspended by a wire through an extremely narrow neck, and it grows longitudinally as it is withdrawn gradually from the molten material. The neck is easily broken due to collision between the monocrystal and the wall of the puller, even during even weak earthquakes. In this study, an active isolation system using linear motors has been developed because the linear motors are the most suitable actuators for this purpose. Through shake table tests, it was shown that the active isolation system could effectively reduce the displacement of the monocrystal model.

INTRODUCTION

Presently, almost all semiconductor devices are made from silicon monocrystal, gallium-arsenic monocrystal, and so on. Further, most of the equipments or machines used currently do not work without electronics. This implies that pursuing efficiency in the monocrystal manufacturing process is very important.

In the case of silicon, for example, about 90% or more of all the silicon monocrystals are grown according to the Czochralski (CZ) method. In the CZ process, the seed crystal is immersed into the melting silicon in the crucible, and then withdrawn slowly. A monocrystal forms on the end of the seed crystal and grows longitudinally as it is withdrawn (shown in Fig. 1). In recent years, the monocrystal, about 300 mm in diameter, is suspended by a wire through an extremely narrow neck, about 5 mm in diameter, in a monocrystal puller. The neck is easily broken due to collision between the monocrystal and the wall of the puller, even during weak earthquakes.

Currently, the passive isolation devices are used to prevent equipment malfunction due to earthquakes. However, in the case of a monocrystal puller, unfortunately, the monocrystal and the wire form a pendulum having a considerably long time period. As a result of this resonance factor, passive isolation

[1] Yacmo Co., Ltd., Tokyo, JAPAN. E-mail: furukawa@yacmo.co.jp
[2] Professor, Institute of Industrial Science, The University of Tokyo, JAPAN.
[3] Associate Professor, Tokyo University of Agriculture and Technology, JAPAN.
[4] Hitachi Medical Corporation, JAPAN.
[5] Postgraduate Student, Tokyo University of Agriculture and Technology, JAPAN.

systems cannot sufficiently reduce the response of the pendulum to the earthquakes. Therefore, an active isolation system is required.

In this study, an active isolation system using linear motors has been developed because the linear motors are the most suitable actuators for this purpose. Shaking table tests were carried out for a one-dimensional experimental model consisting of an isolation device, external size 1950 mm × 1950 mm × 570 mm; a monocrystal puller model, 2025 mm in height and 538 kg in mass; and a monocrystal model, 150 mm in diameter, 450 mm in length and 63kg in mass.

Through shake table tests, it was shown that the active isolation system could effectively reduce the displacement in the monocrystal model. The system can perform as an active-passive seismic isolation system that can provide not only active isolation to protect the monocrystal, under production from weak earthquakes but also passive isolation to protect the puller from strong earthquakes.

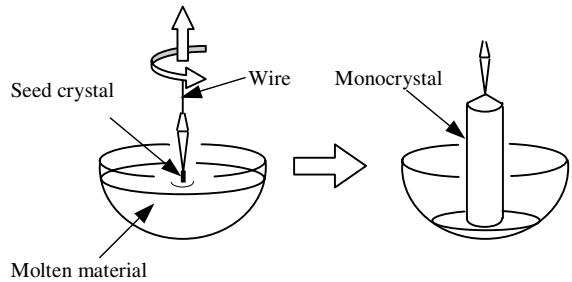

Fig. 1 Growth of a monocrystal (CZ method)

MONOCRYSTAL PULLER MODEL AND ACTIVE ISOLATION DEVICE

The experimental model consists of three portions: a seismic isolation device, a monocrystal puller model, and a monocrystal model. The movable frame of the isolation device is supported by four linear bearings, and is connected to the base frame by a tension spring and a viscous damper. A linear motor is fixed on the base frame and one end of the column is connected to the movable frame. The maximum displacement of the movable frame is ±245 mm, the natural frequency at the time of all loading is ca. 0.25 Hz, and the attenuation coefficient is ca. 15%. The monocrystal puller model has a cylindrical structure and is 538 kg in mass. The monocrystal model has a pillar form and is 63kg in mass. It is suspended from the top of the monocrystal puller model by a wire cable, 5 mm in diameter. The natural frequency of the pendulum formed by the wire cable and the monocrystal model is ca. 0.4 Hz (shown in Figs. 2 and 3).

Fig. 2 Appearance of the experimental model

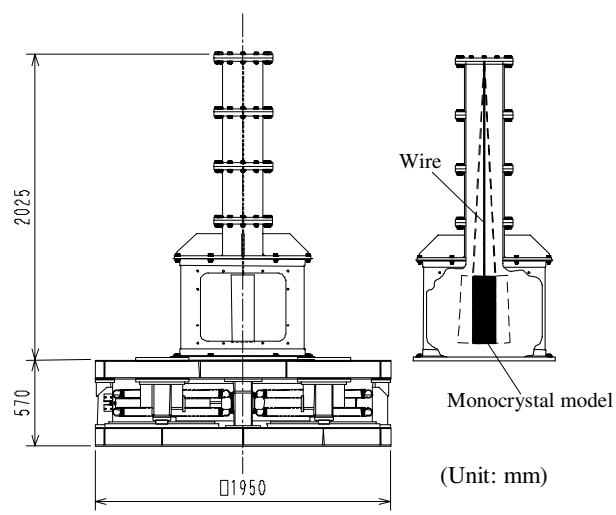

Fig. 3 Schematic diagram of the experimental model

LINEAR MOTOR FOR THIS STUDY

Different types of actuators can be used to manipulate devices. In this study, the linear motor was chosen due to the following reasons:

(1) Its overwhelming simplicity and reliability
(2) Low friction mechanism
(3) Slider activation only on the interception of power supply.

The above-mentioned properties are possible because a linear motor directly converts electrical energy into linear motion, without using complicated mechanisms. A linear motor consists of primary and secondary windings. When powered by a three-phase alternating current, a moving flux is produced in the primary winding. The current induced in the secondary winding reacts with the flux, producing a mechanical force. The interaction of the flux and the current moves the secondary winding linearly.

The linear motor used in this study was originally developed for elevators. The outline is shown in Fig. 4.

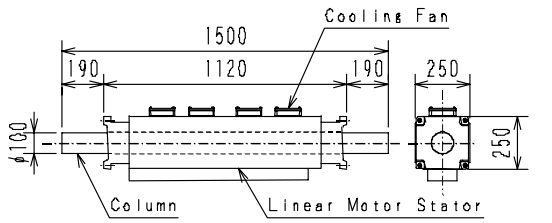

(Unit: mm)

Fig. 4 Schematic diagram of the linear motor

CONTROL SYSTEM

The control system is shown in Fig. 5. The acceleration signal detected by the sensor attached to the isolation device was sent to the DSP through an A/D converter. Then, the command voltage was calculated according to the algorithm designed beforehand, and inputted into the linear motor controller through a D/A converter. In the controller, the optimal current value for the linear motor drive is computed, based on the inputted command voltage and then inputted into the linear motor.

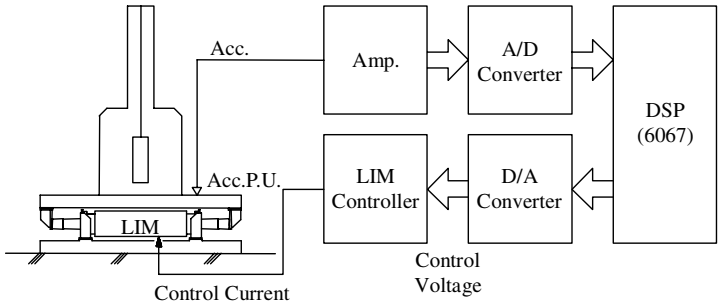

Fig. 5 Control system

ANALYTICAL MODEL

3-mass system model

The analytical model of the monocrystal puller model and the isolation device is shown in Fig. 6. In this study, the system was treated as a 3-mass system of the isolation device, the monocrystal puller model, and the monocrystal model.

The sliding part of the isolation device experiences friction. Therefore, the state of the device is divided into fixation and operation based on the size of the input seismic wave. Here, the equations of motion are expressed as follows, where the fixation state is Phase 1 and the operation state is Phase 2.

Phase 1: In case the isolation device is fixed by friction

$$m_2\ddot{x}_2 + (c_2 + c_3)\dot{x}_2 - c_3\dot{x}_3 - k_2x_1 + (k_2 + k_3)x_2 - k_3x_3 = -m_2\ddot{z}$$
$$m_3\ddot{x}_3 - c_3\dot{x}_2 + c_3\dot{x}_3 - k_3x_2 + k_3x_3 = -m_3\ddot{z}$$
$$(\ x_1 = const\ ,\ \dot{x}_1 = 0\ ) \qquad \cdots\cdots\cdots (1)$$

Phase 2: In case the isolation device is operating

$$m_1\ddot{x}_1 + (c_1 + c_2)\dot{x}_1 - c_2\dot{x}_2 + (k_1 + k_2)x_1 - k_2x_2 = -sign(\dot{x}_1)\mu(m_1 + m_2 + m_3) - m_1\ddot{z}$$
$$m_2\ddot{x}_2 - c_2\dot{x}_1 + (c_2 + c_3)\dot{x}_2 - c_3\dot{x}_3 - k_2x_1 + (k_2 + k_3)x_2 - k_3x_3 = -m_2\ddot{z}$$
$$m_3\ddot{x}_3 - c_3\dot{x}_2 + c_3\dot{x}_3 - k_3x_2 + k_3x_3 = -m_3\ddot{z} \qquad \cdots\cdots\cdots (2)$$

The conditions for phase change are as follows:

○Phase 1→Phase 2

$$\left|m_1\ddot{z} - c_2\dot{x}_2 + (k_1 + k_2)x_1 - k_2x_2\right| > \mu(m_1 + m_2 + m_3)g \qquad \cdots\cdots\cdots (3)$$

○Phase 2→Phase 1

$$\dot{x}_1 = 0 \quad \text{and}$$
$$\left|m_1(\ddot{x}_1 + \ddot{z}) - c_2\dot{x}_2 + (k_1 + k_2)x_1 - k_2x_2\right| \le \mu(m_1 + m_2 + m_3)g \qquad \cdots\cdots\cdots (4)$$

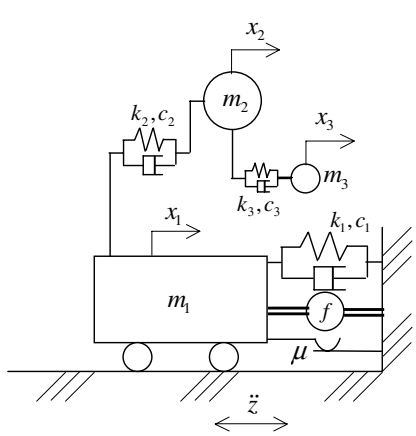

Fig. 6 Analytical model

Identification of the analytical model

To measure the mass of the experimental equipment, the mass was divided into three components and the mass of each component was measured separately. Next, a sweep wave of about frequency bands of 0.1–20 [Hz] was inputted using the shaking table, and the response of the isolation device and the monocrystal puller model was measured. Each parameter was determined based on a response result and the movement equations of the analysis model.

The identified parameters are shown in Table.1.

Table.1 Identified parameters

Mass [kg]		Stiffness coefficient [N/m]		Attenuation coefficient [Ns/m]		Friction factor	
m_1	853	k_1	2.71e3	c_1	6.18e2	μ	0.006
m_2	247	k_2	2.99e6	c_2	1.09e3		
m_3	63	k_3	3.98e2	c_3	2.22e2		

Identification of dynamic characteristic of the linear motor

The transfer characteristic from command voltage to an output thrust was measured by inputting the sinusoidal wave that minced moderately within the limits of a frequency band 0.1–20 [Hz] as the command signal into the linear motor, and the dynamic characteristic of the linear motor was drawn by curve fitting. The transfer characteristic computed by the experiment result and the dynamic characteristic of the linear motor are shown in Fig. 7.

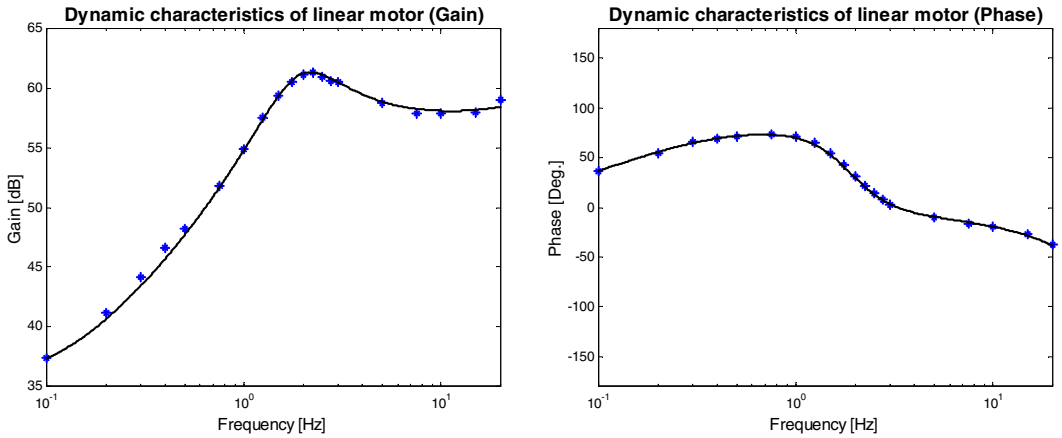

Fig. 7 Dynamic characteristic of the linear motor

CONTROL DESIGN

1-mass system model for control design

In a monocrystal puller, since a silicon monocrystal is in a high temperature state of 1400ºC or above, it is especially difficult to directly measure data, which is required for control. Due to this reason, the controller for a monocrystal puller was built to operate using only one parameter of the acceleration data in the isolation device. Therefore, the movement model for the control system design is a 1-mass system. Moreover, since it was difficult to design a controller for a nonlinear model, the friction of the isolation device was neglected and it was treated as an alignment model. However, when considering attenuation by friction, the influence of fricative is approximated by treating the attenuation coefficient as a larger value than the original value.

$$m_1\ddot{x}_1 + \tilde{c}_1\dot{x}_1 + k_1x_1 = F_a - m_1\ddot{z} \qquad \cdots\cdots\cdots (5)$$

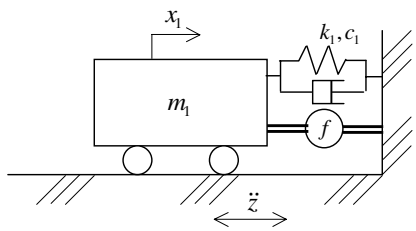

Fig. 8 Analytical model for the control system design

Model matching method

In this study, the controller was designed by the model matching method. As a reference, this method designs a closed loop transfer function based on the transfer function of a plant for visual comprehension, and then it computes the control system that realizes it by reverse operation.

Here, the system shown in Fig. 9 is considered

When this system is set with $y = L(\ddot{x} + \ddot{z}), u = L(u), d = L(\ddot{z})$, y is expressed as follows:

$$y = P_{uy} \cdot u + P_{dy} \cdot d \qquad \cdots\cdots\cdots (6)$$

Here, P_{uy} is an open loop transfer function from a control input to an output, and P_{dy} is the disturbance to the plant. Moreover, when C_{yu} is converted into an open loop transfer function from an output to a control input and C_{ru} is converted into the target value of a controller, W_{ry}, W_{vy}, and, W_{dy}, which show the target value, the observation noise, and the closed loop transfer function from disturbance to an output are expressed as follows:

$$W_{ry} = (1 - P_{uy}C_{yu})^{-1}P_{uy}C_{ru} \qquad \cdots\cdots\cdots (7)$$

$$W_{vy} = (1 - P_{uy}C_{yu})^{-1}P_{uy}C_{yu} \qquad \cdots\cdots\cdots (8)$$

$$W_{dy} = (1 - P_{uy}C_{yu})^{-1}P_{dy} \qquad \cdots\cdots\cdots (9)$$

To ensure adequate controller design by the model matching method, W_{ry} and W_{vy} must satisfy the following three conditions.

(1) Realization conditions

⇒The relative degree of W_{ry} and W_{vy} is larger than the relative degree of P_{uy}.

(2) Connection conditions

⇒The zero points of W_{ry} and W_{vy} contains all the zero points of P_{uy}.

(3) Degree conditions

⇒The zero points of $(1 + W_{vy})$ contains all the poles of P_{uy}.

Furthermore, it is possible to include the filter characteristic in a controller by providing the dynamic characteristics. The controller is designed by specifying the transfer function W_{dy} from disturbance to an output.

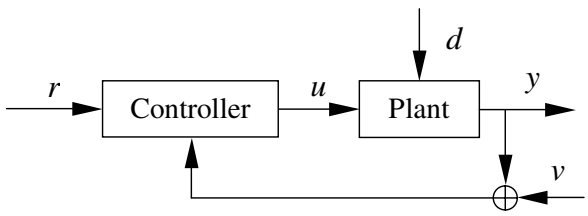

r : *Reference input*

v : *Measurement noise*

u : *Control input to the linear motor*

d : *Disturbance acceleration to the isolator*

y : *Output acceleration of the isolator*

Fig. 9 Block diagram of control system

Determination of parameters of a controller

The system-wide poles determine a controller. The pole details were determined as follows: 2 about an original plant, 1 about a high-pass filter, 2 about a low-pass filter, 4 about a linear motor, and 7 defined arbitrarily. These poles were determined based on the form of W_{dy} and C_{yu}.

W_{dy} and C_{yu} are shown in Figs. 10 and 11.

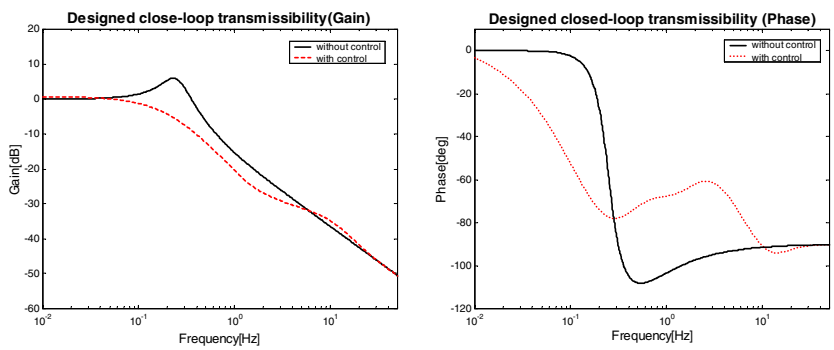

Fig. 10 W_{dy}

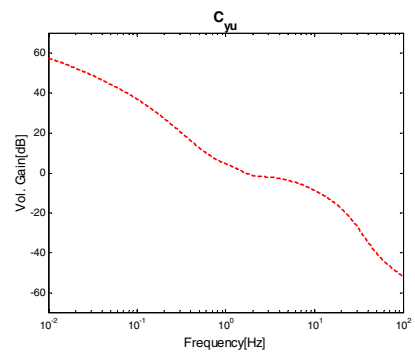

Fig. 11 C_{yu}

EXPERIMENTAL RESULTS

Shaking table tests

In the excitation tests, various earthquake inputs were used including ground motion records from El Centro waves (Imperial Valley Earthquake, 1940) and JMA Kobe waves (Hyougo-ken Nanbu Earthquake, 1995). The peak acceleration of the earthquake inputs was adjusted to 0.1, 0.3, and 0.5 m/s^2.

The length of the wire which suspends the monocrystal model is 1425 mm. Furthermore, the natural frequency of the pendulum, which consists of the monocrystal model and the wire cable, is ca. 0.4 Hz.

In shaking table tests, the tendency of the isolation effects to increase with input acceleration was verified by taking the experimental result into consideration. Therefore, only the experimental result that inputted the peak acceleration of the earthquake inputs as 0.1 and 0.5 m/s^2 are discussed.

Figs. 12 and 13 show the time history displacements of the monocrystal model when non-isolated and isolated by the passive mode and by the active mode, respectively.

When a time history displacement is observed for non-isolated and isolated during the passive modes, there is almost no difference in the amplitude of a monocrystal model. The reason for this is that the natural frequency of the isolation device is not sufficiently low compared with a pendulum. Therefore, the protection for a monocrystal by passive isolation is limited.

On the other hand, active isolation effectively reduces displacement of the monocrystal model.

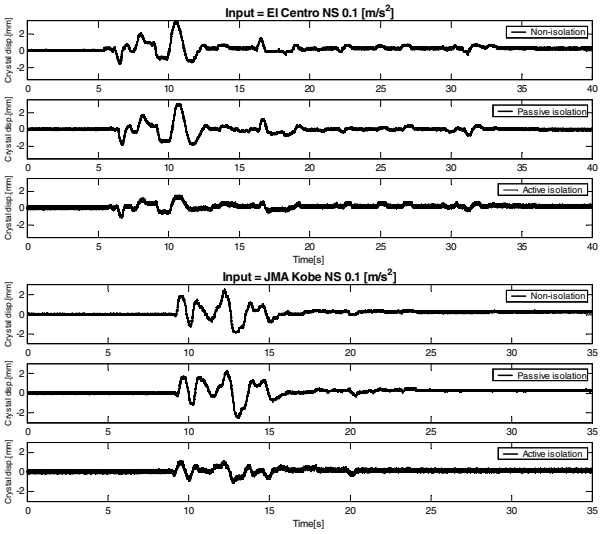

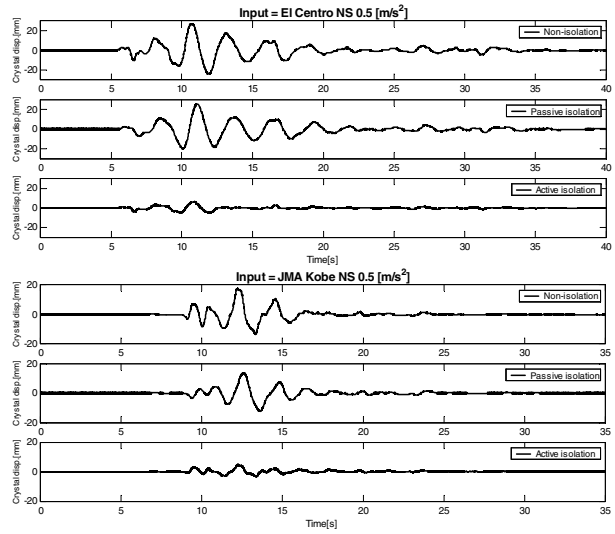

Fig. 12 Displacement of the monocrystal (Input = 0.1 m/s^2) Fig. 13 Displacement of the monocrystal (Input = 0.5 m/s^2)

Robustness

In the monocrystal puller, the natural frequency of the pendulum, which consists of a monocrystal and a wire, changes as the wire pulls up the monocrystal. Therefore, the designed controller must be robust enough so that the seismic isolation performance does not worsen, even if the dynamic characteristic of this pendulum changes. Adjustment of the wire length in three stages approximates the change in the dynamic characteristic of the pendulum accompanying the monocrystal withdrawal process, and the seismic isolation performance of each case was verified. Wire length is Len1 (= 1425 mm), Len2 (= 1065 mm) and Len3 (= 345 mm) in the descending order.

Fig. 14 shows the maximum displacement of the monocrystal model when non-isolated, isolated by the passive mode, and by the active mode, respectively. The controller is designed for Len1. However, on comparing the displacement of the monocrystal model when isolated by the passive mode and the active mode, respectively, irrespective of the wire length the performance of the controller in decreasing the displacement of the monocrystal model was verified as 50% to 77%. Therefore, it can be said that the designed controller in this study has robustness to change in wire length.

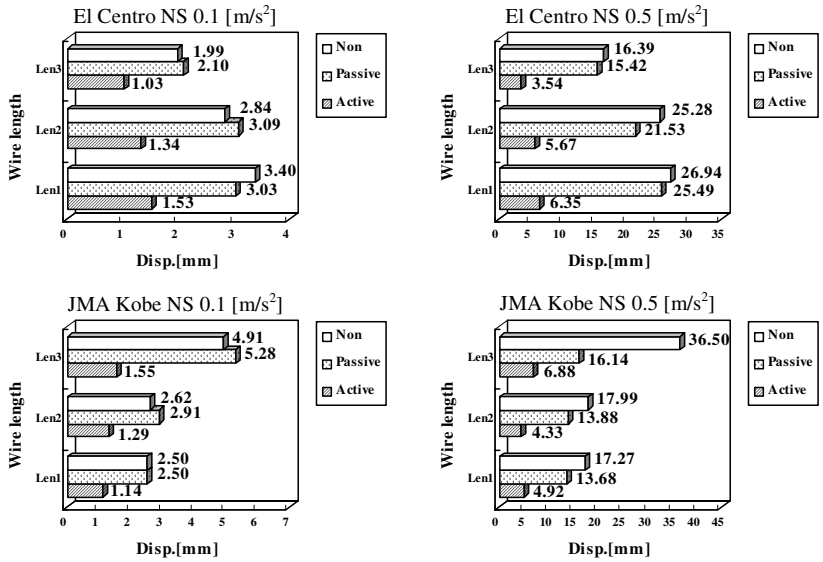

Fig. 14 Maximum displacement of the monocrystal model

Active-Passive mode switching tests

Evidently, when a weak earthquake occurs, the isolation system works as an active isolation device that can effectively protect the monocrystal. Furthermore, the isolation system must change automatically to the passive mode when a strong earthquake, which exceeds the capacity limit of a linear motor, occurs. The active-passive mode switching tests were carried out in order to verify the variation in isolation performance. The peak acceleration of the earthquake inputs was adjusted to 2.0 m/s^2. When the output of the linear motor exceeded the preset value, the isolation system was set up such that the mode is switched from the active to the passive.

The mode-switching rule was determined such that when the command voltage to the linear motor exceeds 1 [V], the mode is switched. Fig. 15 shows the time history displacements of the monocrystal model when isolated by the passive mode alone and by the hybrid mode with the active-passive mode switching, for Len1, Len2, and Len3, respectively.

The test results reveal that when the system functions in active mode, the displacement of the monocrystal model is effectively reduced. On switching to the passive mode, the displacement of the monocrystal model showed a response equivalent to the result of the passive isolation experiment.

Thus, the effectiveness of the active-passive mode switching was verified based on the protection systems for the motor and the driver.

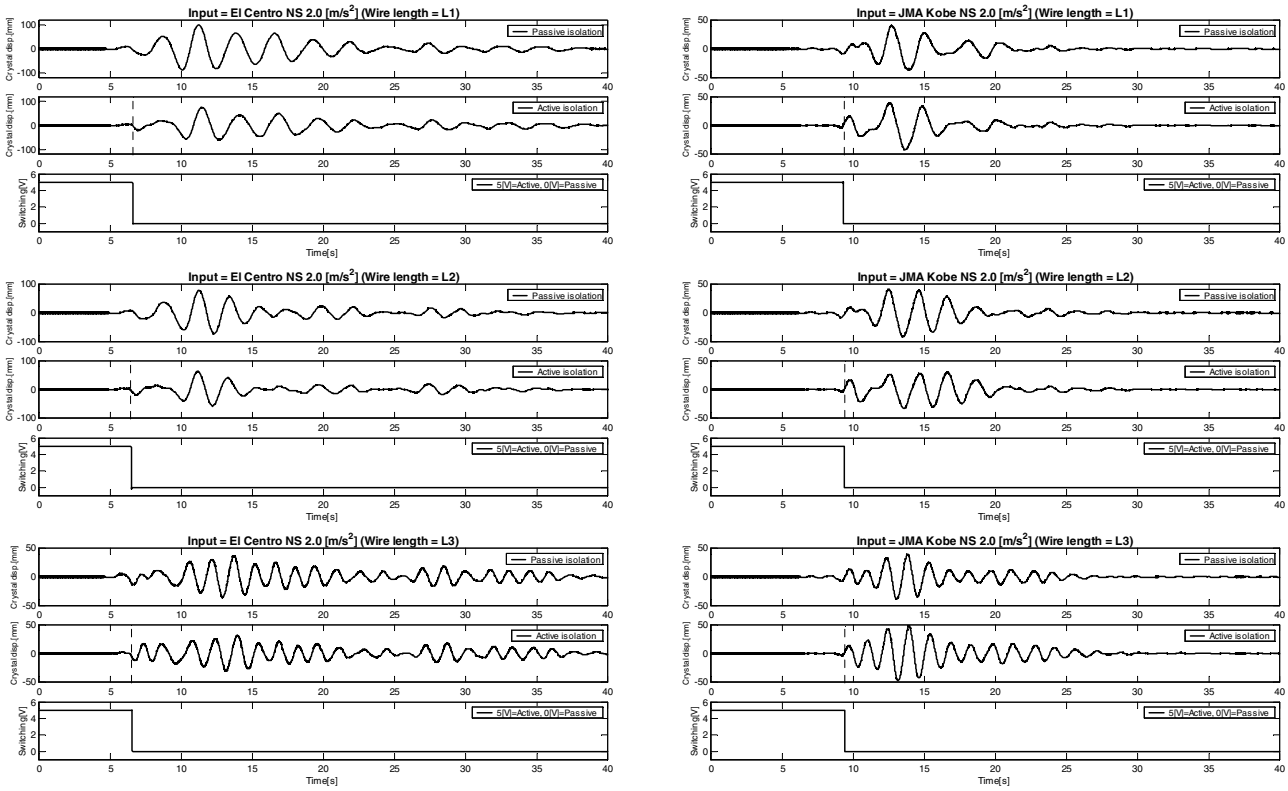

Fig. 15 Excitation experiment with active-passive modes

CONCLUSION

A seismic isolation system with convertible active and passive modes has been developed using a linear motor. The performance of the system was verified by time history displacement of the monocrystal model. The following conclusions are obtained:

(1) A linear motor used in the active isolation system is effective in preventing the collision of the monocrystal resulting from earthquakes.

(2) It was verified that the active isolation system that uses a controller designed by the model matching method, reduces the displacement of a monocrystal.

(3) The effectiveness of the active-passive mode switching was verified based on the protection systems for the motor and the driver.

REFERENCES

1. T. Fujita, Q. Feng, E. Takenaka, T. Takano, and Y. Suizu, "Active Isolation of Sensitive Equipment for Weak Earthquakes," Proceeding of Ninth World Conference on Earthquake Engineering, Vol.8, SE-10 (1988).
2. T. Fujita, Y. Tagawa, N. Murai, S. Shibuya, A. Takeshita, and Y. Takahashi, "Study of Active Microvibration Control Device Using Piezoelectric Actuator (1st Report, Fundamental Study of One-Dimentional Microvibration Control)," Trans. of the Japan Society of Mechanical Engineers, Vol.57, No.540, Ser. C, (in Japanese) (1991).
3. T. Fujita, K. Tanaka, H. Ohyama, Y. Nakamura, H. Hora, H. Miyano, and M. Suganuma, "Large-Scale Model Experiment of Hybrid Mass Damper with Convertible Active and Passive Modes Using Linear Motor for Vibration Control of Tall Buildings," Trans. of the Japan Society of Mechanical Engineers, Vol.62, No.594, Ser. C, (in Japanese) (1996).
4. T. Fujita, T. Bessho, H. Hora, K. Tanaka and Y. Nakamura, "Control Methods for Active Mass Damper Using Linear Motor for Vibration Control of Tall Buildings," Trans. of the Japan Society of Mechanical Engineers, Vol.64, No.620, Ser. C, (in Japanese) (1998).